

Improvement of Conversion Loss of Resistive Mixers Using Bernal-Stacked Bilayer Graphene

Mengchuan Tian, Xuefei Li¹, Qingguo Gao, Xiong Xiong, Zhenfeng Zhang, and Yanqing Wu¹

Abstract—In this letter, we present dual-gate Bernal-stacked bilayer graphene FETs which are used for gate-pumped resistive mixers. The results show that the conversion loss improves when the device on/off ratio increases. At 2 GHz, a record conversion loss of 12.7 dB has been obtained from 0.16 μm device among graphene resistive mixers. Furthermore, more than 10 dB change of conversion loss has been obtained by adjusting the electric displacement field by dual-gate Voltages. Finally, the high-temperature characteristics of this type of graphene mixer exhibit excellent thermal stability with only 2 dB degradation in conversion loss from 300 to 380 K. This result shows that the Bernal-stacked bilayer graphene mixer is promising for low-loss and high-temperature radio frequency circuit applications.

Index Terms—Bilayer graphene, FETs, resistive mixer, conversion loss, high temperature.

I. INTRODUCTION

SINCE the first report of the graphene-based mixer [1], different types of graphene mixers have been proposed, including ambipolar mixers [1]–[5], resistive mixers [6]–[13], metal-insulator-graphene diode mixers [14], and broadband mixer based on asymmetric two-terminal graphene device [15]. Among the various graphene mixers, the passive gate-pumped resistive mixer has attracted much interest due to its low level of undesired intermodulation products and virtually zero dc power consumption. Up to now, the typical conversion loss (CL) of the gate-pumped graphene resistive subharmonic mixers is in the range of 18–31 dB at different operation frequencies [7]–[9], [13]. Moon *et al.* [10] reported an IIP3 of 27 dBm and a CL of 14 dB at 2 GHz based on a gate-pumped fundamental graphene resistive mixer. Lyu *et al.* [11] demonstrated an IIP3 of 21 dBm and a CL of 33 dB at 3.5 GHz by using a double-balanced graphene gate-pumped resistive mixer integrated circuit. Despite impressive progress on the linearity of the resistive mixer, achieving a low CL remains a challenge.

Manuscript received November 15, 2018; revised December 10, 2018 and December 18, 2018; accepted December 18, 2018. Date of publication December 21, 2018; date of current version January 31, 2019. This work was supported in part by the National Natural Science Foundation of China under Grant 61574066 and Grant 61390504, and in part by the Key Basic Research Program of Hubei Province under Grant 2017AAA127. The review of this letter was arranged by Editor S. J. Koester. (Corresponding author: Yanqing Wu.)

The authors are with the Wuhan National High Magnetic Field Center, School of Optical and Electronic Information, Huazhong University of Science and Technology, Wuhan 430074, China (e-mail: yqwu@mail.hust.edu.cn).

Color versions of one or more of the figures in this letter are available online at <http://ieeexplore.ieee.org>.

Digital Object Identifier 10.1109/LED.2018.2889153

It is well known that the CL of a gate-pumped resistive mixer is essentially proportional to $1/(\Gamma_{\max} - \Gamma_{\min})^2$, of which Γ is the reflection coefficient expressed as $(R_{\text{ds}} - Z_0)/(R_{\text{ds}} + Z_0)$ [16]. The R_{ds} is drain-source channel resistance and Z_0 is circuit embedding impedance. To obtain a low CL, the on-state of the channel resistance should be as small as possible to make the optimal impedance $Z_{\text{opt}} = (R_{\max} R_{\min})^{1/2}$ close to Z_0 [7], [9]. On the other hand, a high channel resistance is also needed through gate voltage control, indicating the necessity of a high on/off ratio, which is defined as R_{\max}/R_{\min} . It has been proven that the theoretical CL of resistive mixers improves with increasing on/off ratio and reaches saturation with on/off ratio approaching 100 in traditional semiconductors [16]. To date, however, all resistive graphene mixers are based on zero-bandgap monolayer graphene (MLG) which suffers from a small on/off ratio. In order to obtain a higher on/off ratio and proper impedance levels, some have proposed a new type of graphene device channel which is patterned in the form of an array of bow-tie structures [9]. Although the maximum on/off ratio of 7 has been obtained through the complex fabrication process, it is still not large enough to obtain a desirable low loss resistive mixer. In contrast to the MLG, Bernal-stacked bilayer graphene (BLG) shows a tunable bandgap under a vertically applied electric field, exhibiting a high on/off ratio [17], which holds great potential for low-loss resistive mixers.

In this letter, we have carried out in-depth characterization on the Bernal-stacked BLG resistive mixers for the first time. Starting with the Bernal-stacked BLG growth by chemical vapor deposition (CVD) process, we then characterize the CL of the BLG FET mixers versus on/off ratio for different gate length devices. Subsequently, the dependence of CL on the gate voltage has also been studied. Finally, high-temperature characteristics up to 380 K of this type graphene mixer have been demonstrated. Our work provides a new method to obtain resistive mixers with low CL for potential utilization of CVD graphene in microwave electronics.

II. BLG GROWTH AND CHARACTERIZATION

BLG films were synthesized by the CVD process using a copper pocket method [18]. The BLG growth and transfer process are following the method in our early work [5] and is summarized as follows: first, the growth system was heated to 1070 °C under an H_2 flow of 100 sccm and annealed for 120 min. Subsequently, CH_4 and H_2 were introduced into the system for BLG growth at flow rates of 0.5 sccm and 60 sccm, respectively. Finally, the graphene films outside the copper pocket were transferred onto a SiO_2/Si substrate

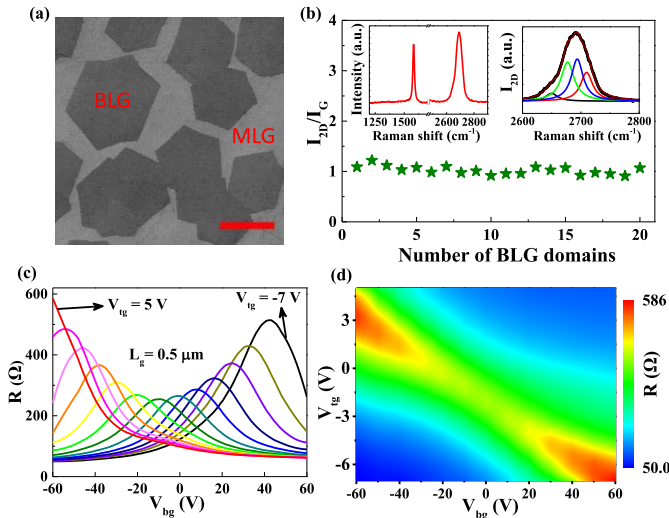


Fig. 1. (a) SEM photograph of the transferred graphene film. Scale bar, 40 μm . (b) The intensity ratios of the 2D peak and G peak from the Raman spectroscopy of 20 BLG domains. Two insets represent the Raman spectra of a BLG domain and its 2D peak fitting. (c) Resistance as a function of V_{bg} at different V_{tg} . The V_{ds} is fixed at 0.1 V. (d) Two-dimensional plot of resistivity in c.

covered with a 14 nm atomic layer deposited (ALD) high- k HfSiO dielectric, which was deposited at 300 °C followed by rapid thermal annealing at 650 °C in nitrogen ambient. The HfSiO film shows crystallization and the content of Si and Hf atomic in the HfSiO film is about 5 % and 20 %, respectively. Also, the HfSiO dielectric with a dielectric constant of 18 is expected to screen the charged impurities located in proximity to the channel layer, which results in better carrier mobility [19], [20]. A scanning electron microscopy (SEM) image of the transferred graphene film is shown in Fig. 1(a), where BLG domains as large as 100 μm can be obtained. Raman spectroscopy was used to characterize the Bernal-stacked nature of the BLG domains, as shown in Fig. 1(b). The intensity ratios of the 2D peak and G peak for 20 representative BLG domains are all near 1 as expected. The two insets in Fig. 1(b) show the Raman spectrum of a BLG domain (left) and its 2D peak fitted with four Lorentz peaks (right), corresponding to the characteristics of Bernal-stacked BLG [21]. Dual-gate RF transistors with ground-signal-ground (GSG) coplanar pad design were fabricated [5]. Both electron-beam lithography (EBL) and electron-beam evaporation (EBE) processes were used to define the channel (20 μm width), source and drain contacts (20 nm Pd/60 nm Au), and the gate electrodes (20 nm Ni/60 nm Au). For top-gate dielectrics, 2 nm Al was first deposited by the EBE as a seed layer which was oxidized subsequently, and then 15 nm Al_2O_3 was deposited by ALD at 300 °C. All our devices were fabricated on single crystalline BLG domains to avoid the scattering effect of grain boundaries.

Fig. 1(c) shows the channel resistance as a function of the back-gate voltage (V_{bg}) and top-gate voltage (V_{tg}) at a fixed drain voltage (V_{ds}) 0.1 V with a 0.5 μm long BLG FET. All the measurements were carried out in a vacuum environment. Fig. 1(d) shows the two-dimensional color plot of channel resistance in Fig. 1(c). The off-resistance increases in both directions of back-gate voltage away from Dirac point, which

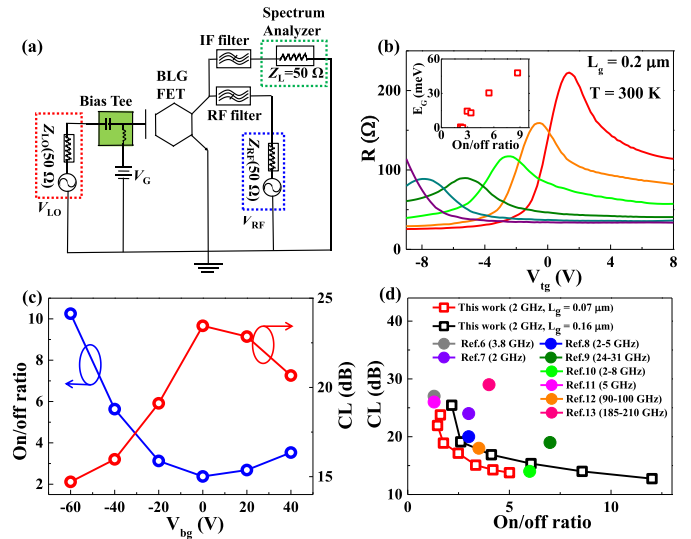


Fig. 2. (a) Measurement setup for the gate-pumped BLG FET resistive mixer. (b) Channel Resistance as a function of V_{tg} at different V_{bg} with $V_{\text{ds}} = 0.1$ V. The inset shows extracted energy bandgap (E_{G}) versus on/off ratio. (c) The mixer on/off ratio and CL versus V_{bg} for the 0.2 μm long device. (d) The mixer CL versus on/off ratio for our results and those in references.

is also consistent with previous reports on Bernal-stacked BLG devices [17].

III. CONVERSION LOSS OF RESISTIVE MIXER

Fig. 2(a) shows a schematic view of the gate-pumped resistive BLG FET mixer test circuit. The external high pass RF filter and low pass intermediate frequency (IF) filter are used to separate the RF signal (2.2 GHz) applied to the drain port and the IF signal (200 MHz) extracted from the drain port, respectively. The two filters provide good port isolation which is more than 40 dB for both LO-IF and RF-IF port. The applied local oscillator (LO) signal power and frequency is 15 dBm and 2 GHz, respectively. Fig. 2(b) shows the channel resistance as a function of V_{tg} at different V_{bg} for a 0.2 μm long BLG FET with $V_{\text{ds}} = 0.1$ V. The inset in Fig. 2(b) shows extracted energy bandgap (E_{G}) versus on/off ratio using the method described in previous report [22]. The bandgap at $V_{\text{bg}} = -60$ V is estimated to be 47 meV. This relatively small bandgap can be attributed to the more charge carrier inhomogeneities in wide channel ($W = 20$ μm) and thick top-gate dielectric in our devices [23]. Fig. 2(c) shows the dependence of CL and on/off ratio on the V_{bg} . When the V_{bg} changes, the CL and on/off ratio have an exactly opposite tendency. Fig. 2(d) shows the relationship between CL and on/off ratio for our results together with those in references. As expected, the CL decreases with increasing on/off ratio. The minimal CL is 12.7 dB for the 0.16 μm device, which is the lowest CL at few gigahertz frequencies compared with the reported single graphene-based FET resistive mixers. Moreover, CL changes more than 10 dB for 0.07 and 0.16 μm long devices over the operation voltage range, indicating a significant tunable effect of the CL by the dual-gate voltage. Noteworthy, short channel devices show a lower CL at high on/off ratios compared to the long channel device, which can be attributed to a better Z_{opt} for the short

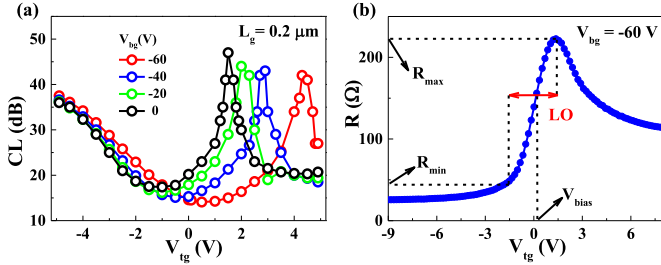


Fig. 3. (a) CL versus the V_{tg} at different V_{bg} . (b) Explanation the CL dependence on V_{tg} at fixed LO power of 15 dBm (about 3 V sweeping range).

channel device. At the on/off ratio of about 4, the Z_{opt} is about 115 Ω and 48 Ω for the 0.16 μm and 0.07 μm devices, respectively. The Z_{opt} for the short channel device is closer to $Z_0 = 50 \Omega$ thus leading to a lower CL. This result suggests a significant advantage of the short channel Bernal-stacked BLG devices with high on/off ratio for the low-loss resistive mixers. The performance of the mixer can be further improved by using higher mobility or higher charge density graphene materials, where low on-state resistance can be obtained for optimal Z_{opt} closer to Z_0 . In addition, we also measured the dependence of the CL on the top-gate voltage applied to the gate port, as shown in Fig. 3(a). It is noted that a minimum CL can be obtained under optimal bias point which depends on the channel interface quality, where minimal hysteresis in the transfer characteristics is highly desired. Fig. 3(b) explains the dependence of CL on top-gate bias voltage at fixed LO power. For a fixed LO power level, the gate swing voltage range remains the same. The R_{max} and R_{min} change with the shift of the bias point, thus resulting in the CL change. A large LO power is necessary to properly pump the resistive mixer device between the ON and OFF states. Thinner dielectric and high- k materials can be used for gate dielectric to reduce the LO power.

IV. HIGH TEMPERATURE CHARACTERISTICS

The ability to operate devices at high temperatures has proven crucial for reliability assessment. To evaluate the performance of the gate-pumped graphene resistive mixer with varying temperatures, we measured the mixer performance as a function of temperature up to $T = 380 \text{ K}$. Fig. 4(a) shows the channel resistance as a function of V_{tg} at different V_{bg} for the 0.2 μm long device at $T = 380 \text{ K}$. Both on-resistance and off-resistance are increasing with increasing the temperature. The maximum on/off ratio is about 5 at $T = 380 \text{ K}$ and $V_{bg} = -60 \text{ V}$. Fig. 4(b) shows the dependence of CL and on/off ratio on the temperature. When the temperature increases, the on/off is decreasing and results in degradation of the CL. It can be seen that the CL increases by only 2 dB as the temperature increases from 300 to 380 K. Fig. 4(c) shows the mixer IF output power versus the RF input power (RF_{in}) at $V_{bg} = -60 \text{ V}$. The input 1-dB compression point decreases from about 2.5 dBm at 300 K to about 1.5 dBm at 380 K. The inset in Fig. 4(c) shows the time dependent measurement of the CL at 380 K. There is about 2 dB degradation of CL after three hours. Fig. 4(d) shows the CL of the mixer versus LO power. As can be seen, the CL decreases

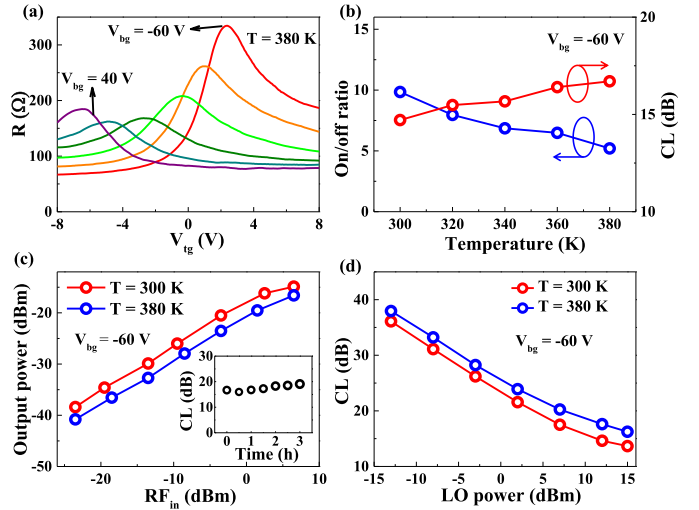


Fig. 4. (a) The channel resistance as a function of V_{tg} at different V_{bg} for the 0.2 μm BLG FET at 380 K. (b) The mixer on/off ratio and CL versus temperature. (c) Measured IF output power versus RF input power. Inset shows long-term thermal stability at 380 K. (d) Measured CL versus LO power.

TABLE I

COMPARISON OF SINGLE GRAPHENE FET RESISTIVE MIXERS

Ref.	Scheme	On/off ratio	f_{RF} (GHz)	CL (dB)	Temperature (K)
[6]	Epitaxial	1.3	3.8	27	300
				28	400
[7]	Exfoliated	3	2	24	300
[8]	Exfoliated	3	2-5	20-22	300
[9]	Exfoliated	7	24-31	19 \pm 1	300
[10]	Epitaxial	6	2-8	14-14.5	300
[11]	CVD	1.3	5	26	300
[12]	Epitaxial	3.5	90-100	18	300
[13]	CVD	4	185-210	29 \pm 2	300
				29 \pm 2	300
This work	CVD BLG	12	2.2	12.7	300
		10	2.2	14.7	300
		5	2.2	16.7	380

linearly with LO power up to the onset of saturation at about 15 dBm.

Table I summarizes the measured performance of the BLG FET mixer and the comparison with other single graphene-based resistive mixers. It is clear that the on/off ratio maximum and CL minimum of our BLG FET mixer outperform other results. The minimal CL of the BLG FET mixer is also better than metal-insulator-graphene diode mixer (15 dB) [14] and asymmetric two-terminal graphene broadband RF heterodyne mixer (27 \pm 3 dB) [15].

V. CONCLUSION

In conclusion, the radio frequency characteristics of the Bernal-stacked BLG gate-pumped resistive FET mixers have been presented for the first time. The high on/off ratio of 12 by a perpendicularly electric displacement field results in a record CL of 12.7 dB. Also, the mixer exhibits relatively good thermal stability with a 2 dB increase in CL from 300 to 380 K. The reported Bernal-stacked BLG FET mixer performance provides important guidelines to obtain high-performance low power consumption graphene resistive mixers.

REFERENCES

- [1] H. Wang, A. Hsu, J. Wu, J. Kong, and T. Palacios, "Graphene-based ambipolar RF mixers," *IEEE Electron Device Lett.*, vol. 31, no. 9, pp. 906-908, Jul. 2010, doi: 10.1109/LED.2010.2052017.

- [2] H. Madan, M. J. Hollander, M. LaBella, R. Cavallero, D. Snyder, J. A. Robinson, and S. Datta, "Record high conversion gain ambipolar graphene mixer at 10 GHz using scaled gate oxide," in *IEDM Tech. Dig.*, San Francisco, CA, USA, Dec. 2012, pp. 4.3.1–4.3.4.
- [3] Q. Gao, X. Li, M. Tian, X. Xiong, Z. Zhang, and Y. Wu, "Short-channel graphene mixer with high linearity," *IEEE Electron Device Lett.*, vol. 38, no. 8, pp. 1168–1171, Aug. 2017, doi: [10.1109/LED.2017.2718732](https://doi.org/10.1109/LED.2017.2718732).
- [4] C.-H. Yeh, Y.-W. Lain, Y.-C. Chiu, C.-H. Liao, D. R. Moyano, S. S. H. Hsu, and P.-W. Chiu, "Gigahertz flexible graphene transistors for microwave integrated circuits," *ACS Nano*, vol. 8, no. 8, pp. 7663–7670, Aug. 2014, doi: [10.1021/nn5036087](https://doi.org/10.1021/nn5036087).
- [5] M. Tian, X. Li, T. Li, Q. Gao, X. Xiong, Q. Hu, M. Wang, X. Wang, and Y. Wu, "High performance CVD bernal-stacked bilayer graphene transistors for amplifying and mixing signals at high frequencies," *ACS Appl. Mater. Interfaces*, vol. 10, no. 24, pp. 20219–20224, May 2018, doi: [10.1021/acsami.8b04065](https://doi.org/10.1021/acsami.8b04065).
- [6] Y.-M. Lin, A. Valdes-Garcia, S.-J. Han, D. B. Farmer, I. Meric, Y. Sun, Y. Wu, C. Dimitrakopoulos, A. Grill, P. Avouris, and K. A. Jenkins, "Wafer-scale graphene integrated circuit," *Science*, vol. 332, no. 6035, pp. 1294–1297, Jun. 2011, doi: [10.1126/science.1204428](https://doi.org/10.1126/science.1204428).
- [7] O. Habibpour, S. Cherednichenko, J. Vukusic, K. Yhland, and J. Stake, "A subharmonic graphene FET mixer," *IEEE Electron Device Lett.*, vol. 33, no. 1, pp. 71–73, Jan. 2012, doi: [10.1109/LED.2011.2170655](https://doi.org/10.1109/LED.2011.2170655).
- [8] M. A. Andersson, O. Habibpour, J. Vukusic, and J. Stake, "Resistive graphene FET subharmonic mixers: Noise and linearity assessment," *IEEE Trans. Microw. Theory Techn.*, vol. 60, no. 12, pp. 4035–4042, Dec. 2012, doi: [10.1109/TMTT.2012.2221141](https://doi.org/10.1109/TMTT.2012.2221141).
- [9] O. Habibpour, J. Vukusic, and J. Stake, "A 30-GHz integrated subharmonic mixer based on a multichannel graphene FET," *IEEE Trans. Microw. Theory Techn.*, vol. 61, no. 2, pp. 841–847, Feb. 2013, doi: [10.1109/TMTT.2012.2236434](https://doi.org/10.1109/TMTT.2012.2236434).
- [10] J. S. Moon, H. C. Seo, M. Antcliff, D. Le, C. McGuire, A. Schmitz, L. O. Nyakiti, D. K. Gaskill, P. M. Campbell, K.-M. Lee, and P. Asbeck, "Graphene FETs for zero-bias linear resistive FET mixers," *IEEE Electron Device Lett.*, vol. 34, no. 3, pp. 465–467, Mar. 2013, doi: [10.1109/LED.2012.2236533](https://doi.org/10.1109/LED.2012.2236533).
- [11] H. Lyu, H. Wu, J. Liu, Q. Lu, J. Zhang, X. Wu, J. Li, T. Ma, J. Niu, W. Ren, H. Cheng, Z. Yu, and H. Qian, "Double-balanced graphene integrated mixer with outstanding linearity," *Nano Lett.*, vol. 15, pp. 6677–6682, Sep. 2015, doi: [10.1021/acs.nanolett.5b02503](https://doi.org/10.1021/acs.nanolett.5b02503).
- [12] O. Habibpour, Z. S. He, W. Strupinski, N. Rorsman, T. Ciuk, P. Ciepielewski, and H. Zirath, "A W-band MMIC resistive mixer based on epitaxial graphene FET," *IEEE Microw. Wireless Compon. Lett.*, vol. 27, no. 2, pp. 168–170, Feb. 2017, doi: [10.1109/LMWC.2016.2646998](https://doi.org/10.1109/LMWC.2016.2646998).
- [13] M. Andersson, Y. Zhang, and J. Stake, "A 185–215-GHz subharmonic resistive graphene FET integrated mixer on silicon," *IEEE Trans. Microw. Theory Techn.*, vol. 65, no. 1, pp. 165–172, Jan. 2017, doi: [10.1109/TMTT.2016.2615928](https://doi.org/10.1109/TMTT.2016.2615928).
- [14] M. Saeed, A. Hamed, Z. Wang, M. Shaygan, D. Neumaier, and R. Negra, "Metal-insulator-graphene diode mixer based on CVD graphene-on-glass," *IEEE Electron Device Lett.*, vol. 39, no. 7, pp. 1104–1107, Jul. 2018, doi: [10.1109/LED.2018.2838451](https://doi.org/10.1109/LED.2018.2838451).
- [15] J. Tong, M. C. Conte, T. Goldstein, S. K. Yngvesson, J. C. Bardin, and J. Yan, "Asymmetric two-terminal graphene detector for broadband radiofrequency heterodyne-and self-mixing," *Nano Lett.*, vol. 18, no. 6, pp. 3516–3522, Jul. 2018, doi: [10.1021/acs.nanolett.8b00574](https://doi.org/10.1021/acs.nanolett.8b00574).
- [16] K. Yhland, "Simplified analysis of resistive mixers," *IEEE Microw. Wireless Compon. Lett.*, vol. 17, no. 8, pp. 604–606, Aug. 2007, doi: [10.1109/LMWC.2007.901785](https://doi.org/10.1109/LMWC.2007.901785).
- [17] J. B. Oostinga, H. B. Heersche, X. Liu, A. F. Morpurgo, and L. M. K. Vandersypen, "Gate-induced insulating state in bilayer graphene devices," *Nature Mater.*, vol. 7, no. 2, pp. 151–157, Feb. 2008, doi: [10.1038/nmat2082](https://doi.org/10.1038/nmat2082).
- [18] Y. Hao, L. Wang, Y. Liu, H. Chen, X. Wang, C. Tan, S. Nie, J. W. Suk, T. Jiang, T. Liang, J. Xiao, W. Ye, C. R. Dean, B. I. Yakobson, K. F. McCarty, P. Kim, J. Hone, L. Colombo, and R. S. Ruoff, "Oxygen-activated growth and bandgap tunability of large single-crystal bilayer graphene," *Nature Nanotechnol.*, vol. 11, no. 5, pp. 426–431, Feb. 2016, doi: [10.1038/nnano.2015.322](https://doi.org/10.1038/nnano.2015.322).
- [19] T. Li, Z. Zhang, X. Li, M. Huang, S. Li, S. Li, and Y. Wu, "High field transport of high performance black phosphorus transistors," *Appl. Phys. Lett.*, vol. 110, no. 16, p. 163507, Apr. 2017, doi: [10.1063/1.4982033](https://doi.org/10.1063/1.4982033).
- [20] T. Gao, X. Li, X. Xiong, M. Huang, T. Li, and Y. Wu, "Optimized transport properties in lithium doped black phosphorus transistors," *IEEE Electron Device Lett.*, vol. 39, no. 5, pp. 769–772, May 2018, doi: [10.1109/LED.2018.2820841](https://doi.org/10.1109/LED.2018.2820841).
- [21] A. C. Ferrari, J. C. Meyer, V. Scardaci, C. Casiraghi, M. Lazzeri, F. Mauri, S. Piscanec, D. Jiang, K. S. Novoselov, S. Roth, and A. K. Geim, "Raman spectrum of graphene and graphene layers," *Phys. Rev. Lett.*, vol. 97, no. 18, p. 187401, Nov. 2006, doi: [10.1103/physrevlett.97.187401](https://doi.org/10.1103/physrevlett.97.187401).
- [22] B. N. Szafranek, G. Fiori, D. Schall, D. Neumaier, and H. Kurz, "Current saturation and voltage gain in bilayer graphene field effect transistors," *Nano Lett.*, vol. 12, no. 3, pp. 1324–1328, 2012, doi: [10.1021/nl2038634](https://doi.org/10.1021/nl2038634).
- [23] T. Chu and Z. Chen, "Achieving large transport bandgaps in bilayer graphene," *Nano Res.*, vol. 8, no. 10, pp. 3228–3236, Oct. 2015, doi: [10.1007/s12274-015-0823-x](https://doi.org/10.1007/s12274-015-0823-x).